International Journal on Magnetic Particle Imaging
Vol 6, No 2, Suppl 1, Article ID 2009061, 3 Pages

Infinite Science Publishing

Proceedings Article

HYPER localized hyperthermia – early results

M. Weber[1,*]· D. Hensley[1]· B. Kettlewell[1]· A. Mark[1]· R. Orendorff[1]· M. Peters[1]· B. Tiret[1]· E. Yu[1]· P. Goodwill[1]

[1]Magnetic Insight, Alameda, CA, USA
[*]Corresponding author, email: mweber@magneticinsight.com

Abstract

In magnetic fluid hyperthermia (MFH), Magnetic Nanoparticles (MNPs) dissipate heat when exposed to alternating magnetic fields (AMF). MFH is used for targeted energy deposition for targeted drug-delivery or cancer therapy. To avoid heat deposition in all areas with high particle concentration, a gradient field featuring a field-free area (FFR) can be utilized to isolate heating a target region. In this work, we present preliminary results with a localized hyperthermia system, HYPER, that features a mechanically actuated gradient that enables adjusting the heating region's size and position. The size of the heating region in our prototype is verified by measuring the full width at half maximum (FWHM) of the specific absorption rate (SAR) point spread function (PSF) and compared to a theoretical heating model (1).

I Introduction

Magnetic Fluid Hyperthermia (MFH) has been used for diverse applications that include treating prostate cancer [2], [3], treating brain cancer [4], and controlled drug delivery applications [5]. Typically, MFH in biological applications exposes Magnetic Nanoparticles (MNPs) to strong (>10 mT), rapid (>150 kHz) alternating magnetic fields (AMFs) that causes the MNPs to dissipate heat. Typically, the AMF is generated by an RF coil, known as a work coil, that is sized to the body part being treated, or in preclinical work, surrounds the entire animal. Because all MNPs within the work coil are heated by the AMF, significant off-target MNP heating in the liver and other tissues can occur. This off-target heating can cause unintended effects such as heating the liver or releasing drugs off-target.

Recently, it has been shown that the same gradient fields used in magnetic particle imaging can be used to restrict heating to a small region [6], [7]. In this novel MFH approach, MNPs at the FFR are free to rotate and absorb energy, while MNPs away from the FFR are effectively magnetically "locked," and absorb no more heat than normal tissue.

In this abstract, we present a novel localized hyperthermia system, HYPER, that is suited for small-animal studies. The system featuring mechanically adjustable permanent magnets for both positioning and changing the size of the FFR during heating. The variable gradient enables targeting different treatment region positions and sizes without compromising the surrounding tissue. For example, with a stronger gradient, precise drug release can be accomplished, while weaker gradients can offer whole body MFH applications.

II Material and methods

Here we estimate the Specific Absorption Rate (SAR) using a theoretical model, detail the hyperthermia prototype setup, perform heating experiments, and compare our heating experiments with our theoretical model.

II.I Theoretical Energy Dissipation Model

Simulation results in this work are based on models presented by Soto-Aquino et al. from [1]. The following section summarizes their primary results.

The rate of energy dissipation is often described as the product of magnetic field and magnetization

$$Q = \mu_0 \int_0^{2p} \mathbf{H} \frac{d\mathbf{M}}{dt} dt\,. \tag{1}$$

If the sinusoidal magnetic field and magnetization are collinear, (1) can be expanded to the mean rate of energy dissipation

$$[Q] = \frac{\mu_0 H_0 \Omega}{2p} \int_0^{2p} M \sin(\Omega t) dt\,. \tag{2}$$

Here, H_0 is the magnetic field amplitude, Ω the excitation radian frequency and $p = \pi/\Omega$. We can also introduce dimensionless variables $\tilde{M} = M/M_S$, $\tilde{\Omega} = \Omega\tau$, $\tilde{t} = t/\tau$ and $\tilde{p} = \pi/\Omega\tau$ to simplify the equation

$$[Q] = \frac{\mu_0 H_0 M_S \Omega}{2\tilde{p}} \int_0^{2p} \tilde{M} \sin\left(\tilde{\Omega}\tilde{t}\right) d\tilde{t}\,. \tag{3}$$

$[Q]$ can be represented as specific absorption rate (SAR)

$$\mathrm{SAR} = \frac{[Q]}{\phi\rho} \tag{4}$$

with ϕ being the particle volume fraction and ρ the particle density.

We numerically obtain the magnetization $\tilde{M}$ by solving the magnetization relaxation equation of Martsenyuk, Raikher, and Shliomis [1]

$$\frac{d\tilde{M}}{d\tilde{t}} = -\tilde{M}\left(1 - \frac{\alpha}{\mathscr{L}^{-1}(\tilde{M})}\right). \tag{5}$$

With $\mathscr{L}^{-1}(\lambda)$ being the Padé approximant to the inverse Langevin function [8]

$$\mathscr{L}^{-1}(\lambda) = \lambda \frac{3-\lambda^2}{1-\lambda^2} \tag{6}$$

and a the Langevin parameter

$$a = \frac{\pi\mu_0 d^3 M_s H}{6 k_B T}\,. \tag{7}$$

Equation (5) was implemented in Python and solved numerically with the LSODA solver.

II.II Localized hyperthermia prototype

Our hyperthermia prototype uses mechanical movement to adjust the position and size of the FFR in relation to the sample. Two permanent magnets with opposing magnetization direction generate an FFR (see Fig. 1). Each magnet's position is individually adjustable and hence it is possible to vary the gradient strength between 0.6 T/m and 2.4 T/m (x-direction) and shift the FFR from left to right. To shift up and down, both magnets can be moved vertically. The sample is moved in the z- direction. The AMF is generated by a stationary water-cooled solenoid that is matched to 339 kHz. A maximum field amplitude of 14 mT is achieved.

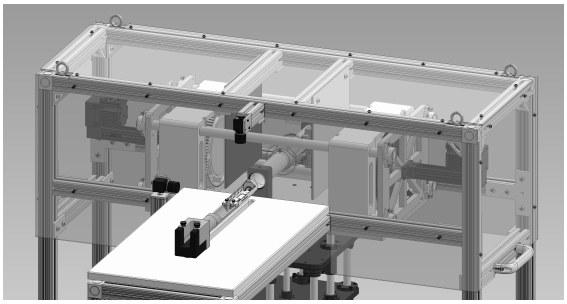

Figure 1: The FFR is generated between two permanent magnets. Both can be individually moved in x-direction to change the gradient strength. A solenoid generates a sinusoidal field at 339 kHz with 14 mT field amplitude.

II.III Heating experiments and data analysis

All measurements were performed with 100 uL synomag®-D (50 nm , 25 mg/mL , 104-00-501, micromod Partikeltechnologie GmbH) filled in a 200 uL PCR tube. The temperature was acquired with a fiberoptic temperature sensor (TS5-20MM-02 and FOTEMP1-OEM-MNT, Micronor). The PCR tube was moved through the FFR with a step size of 5 mm. An AMF was applied for 10 s.

The acquired temperature data was analyzed by identifying the linear loss regime of the temperature curve and applying a linear fit ($\Delta T/\Delta t$) [9]. SAR can be calculated with:

$$\mathrm{SAR} = \frac{C}{m}\frac{\Delta T}{\Delta t} \tag{8}$$

where C is the heat capacity of water (4.18 J/gK) and m the mass of the sample.

III Results and discussion

A maximum SAR of 148 W/g was achieved for the specified experiment. Fig 2. shows the measured and simulated SAR PSF for 0.6 T/m as well as 1.8 T/m. At 0.6 T/m, a FWHM of 46.2 mm is achieved. At 1.8 T/m, the FWHM is reduced to 17.4 mm. The simulated SAR profile agrees well with experimental results.

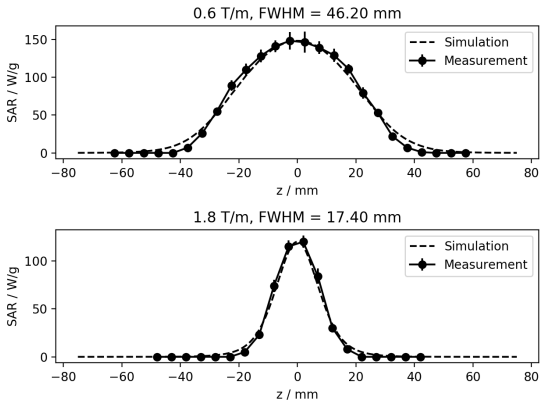

Figure 2: Simulated and measured SAR PSF for synomag®-D with 50 nm hydrodynamic diameter.

IV Conclusions

Here, we presented first results for a localized hyperthermia platform, HYPER, that features a mechanically variable gradient to allow power efficient matching the FFR to the treatment region. Experimental results match the theoretical particle model, and show good agreement between measured SAR values and literature [10]. In the future, we aim to integrate our hyperthermia system into a combined imaging and treatment workflow with the MOMENTUM™ Imager. First, MNP distributions will be determined with MOMENTUM™ and then, selective heating can be applied with HYPER.

Author's Statement

M. Weber, D. Hensley, B. Kettlewell, A. Mark, A. Orendorff, M. Peters, E. Yu and P. Goodwill1are full-time employees for Magnetic Insight, CA, USA. The other authors state no conflict of interest. Informed consent was obtained from all individuals included in this study.

References

[1] D. Soto-Aquino and C. Rinaldi, "Nonlinear energy dissipation of magnetic nanoparticles in oscillating magnetic fields," J. Magn. Magn. Mater., vol. 393, pp. 46–55, 2015.

[2] M. Johannsen et al., "Clinical hyperthermia of prostate cancer using magnetic nanoparticles: Presentation of a new interstitial technique," Int. J. Hyperth., vol. 21, no. 7, pp. 637–647, 2005.

[3] S. Laurent, S. Dutz, U. O. Häfeli, and M. Mahmoudi, "Magnetic fluid hyperthermia: Focus on superparamagnetic iron oxide nanoparticles," Adv. Colloid Interface Sci., vol. 166, no. 1–2, pp. 8–23, 2011.

[4] U. Gneveckow et al., "Description and characterization of the novel hyperthermia- and thermoablation-system MFH®300F for clinical magnetic fluid hyperthermia," Med. Phys., vol. 31, no. 6, pp. 1444–1451, 2004.

[5] C. S. S. R. Kumar and F. Mohammad, "Magnetic nanomaterials for hyperthermia-based therapy and controlled drug delivery," Adv. Drug Deliv. Rev., vol. 63, no. 9, pp. 789–808, 2011.

[6] D. Hensley et al., "Combining magnetic particle imaging and magnetic fluid hyperthermia in a theranostic platform," Phys. Med. Biol., vol. 62, no. 9, pp. 3483–3500, May 2017.

[7] T. Kuboyabu, A. Ohki, N. Banura, and K. Murase, "Usefulness of Magnetic Particle Imaging for Monitoring the Effect of Magnetic Targeting," Open J. Med. Imaging, vol. 06, no. 02, pp. 33–41, 2016.

[8] A. Cohen, "A Padé approximant to the inverse Langevin function," Rheol. Acta, vol. 30, no. 3, pp. 270–273, 1991.

[9] F. Soetaert, S. K. Kandala, A. Bakuzis, and R. Ivkov, "Experimental estimation and analysis of variance of the measured loss power of magnetic nanoparticles," Sci. Rep., vol. 7, no. 1, p. 6661, Dec. 2017.

[10] M. Kallumadil, M. Tada, T. Nakagawa, M. Abe, P. Southern, and Q. A. Pankhurst, "Suitability of commercial colloids for magnetic hyperthermia," J. Magn. Magn. Mater., vol. 321, no. 10, pp. 1509–1513, 2009.

